14th International Conference on Information Fusion
Chicago, Illinois, USA, July 5-8, 2011

# A Novel Sequential Monte Carlo Approach for Extended Object Tracking Based on Border Parameterisation

Nikolay Petrov, Lyudmila Mihaylova, Amadou Gning
School of Computing and Communications
Lancaster University
Lancaster, UK
Emails: {n.petrov,mila.mihaylova,e.gning}@lancs.ac.uk

Donka Angelova
Institute of Information and Communication Technologies
Bulgarian Academy of Sciences
Sofia, Bulgaria
Email: donka@bas.bg

***Abstract*—Extended objects are characterised with multiple measurements originated from different locations of the object surface. This paper presents a novel Sequential Monte Carlo (SMC) approach for extended object tracking based on border parametrisation. The problem is formulated for general nonlinear problems. The main contribution of this work is in the derivation of the likelihood function for nonlinear measurement functions, with sets of measurements belonging to a bounded region. Simulation results are presented when the object is surrounded by a circular region. Accurate estimation results are presented both for the object kinematic state and object extent.**

***Index Terms*—sequential Monte Carlo methods, measurement uncertainty, nonlinear estimation**

## I. Introduction

State estimation for complex stochastic systems, in the presence of non-Gaussian noisy measurements, is of paramount importance for many applications and has been actively investigated during the last decades. One of the most popular state estimation approaches is the Bayesian inference approach [1]–[3]. Within the Bayesian framework the posterior probability density function (pdf) of the state of interest is calculated, conditioned on the available measurements. Among the Bayesian approaches different algorithms have been used, e.g., the Extended Kalman Filter (EKF) [4], Unscented Kalman filter (UKF) [5]–[8] and SMC methods (known as particle filters) [1]–[3], [8], [9]. The Kalman Filter (KF) and its variants such as EKF rely on linearised state and measurement functions, typically up to a first-order Taylor series expansion.

The posterior pdf of the state is approximated by the first two moments of the Gaussian distribution, the mean and covariance of the system state. The UKF [5] avoids linearisation by propagating deterministically chosen points, called sigma points to capture the mean and covariance with a reasonably small set of the carefully selected sigma points. However, both the EKF and the UKF are limited to Gaussian and unimodal type of pdfs. A complex and multimodal pdf can be represented by mixtures of Gaussians as shown in [10]. Using the approximation theory [11], it can be shown that the Gaussian family function is dense in the space of continuous functions and therefore, most of the Kalman type filters have been extended to mixtures of Gaussians.

Particle filtering methods [1]–[3] have recently emerged as a powerful tool for solving complex problems, in the presence of high nonlinearities or/and high dimensional systems, where the propagation of Gaussian mixtures is not always feasible. The particle filtering approach represents the posterior state pdf through samples.

Extended object tracking is an important application where the interest is in finding estimates of the centre of the area surrounding an object and the object extent/size. The extended object usually leads to multiple measurements. Different methods are proposed in the literature for dealing with this problem. Most of the methods separate the problem of kinematic state estimation from the problem of parameter state estimation such as in [12]–[14] and [15]. The extent parameters are estimated separately from the states, for instance with the random matrices approach [12]–[14]. Another group of methods offers a solution to the problem by combining the set-theoretic approach with stochastic fusion [16], [17]. An advantage of the approach proposed in [16] is that neither the measurement source of the extended object, nor the number of measurements are assumed to be drawn from a probability distribution. A comparison between the approach with random matrices and the combined-set theoretic approach is presented in [18]. A SMC approach for extended object tracking is proposed in [19].

In attempt to overcome inherent uncertainties, different interval methods have been proposed, e.g., the method of ellipsoids [20], [21], zonotopes [22]. The interval analysis framework offers promising methodologies for modeling measurements with unknown or complex statistical bounded errors. Initially introduced to propagate rounding errors in mathematical computations earlier in the fifties [23], applications to state estimations have been recently investigated. For instance, in [24], [25] and [26] bounded-error observers, based on a predictor/estimator mechanism combined with various well known interval analysis tools, have been proposed. Other related works are [16], [17], [27]–[32].

In [16] a set-theoretic approach combined with Kalman filtering is proposed for tracking extended objects with a circular disk. Each measurement is originated from an unknown source of the extended object. For this particular problem an interesting solution is proposed, however, it is limited to linear motion models and linear measurement models. In our work we formulate the problem in a broader sense when both the system and measurement models can be nonlinear.

In general the measurement uncertainty can belong to a hypercube or to another spatial shape. In our approach, we consider the general case with a nonlinear measurement equation. The main contributions of the work is in the derived likelihood function based on a parameterised shape and in the developed SMC filter for extended objects. Then we propagate this spatial measurement uncertainty through the Bayesian estimation framework.

The remaining part of this paper is organised in the following way. Section II formulates the problem of interest within the SMC framework. Section III discusses in details the measurement likelihood for the extended object tracking and the parametrisation of the border using a Monte Carlo technique. Examples are included to illustrate the approach. The realisation of the algorithm is presented in Section IV. Results for a circular extended object are shown in Section V. The contributions and open issues for future work are summarised in Section VI.

## II. Extended Object Tracking Within the Sequential Monte Carlo Framework

This work considers the state estimation problem for extended objects. Such objects usually give rise to a set of measurements. The system dynamics and sensor equations are

$$\boldsymbol{x}_k = f(\boldsymbol{x}_{k-1}, \boldsymbol{\eta}_{k-1}), \tag{1}$$

$$\boldsymbol{z}_k = h(\boldsymbol{x}_k, \boldsymbol{w}_k), \tag{2}$$

where $\boldsymbol{x}_k = \left(\boldsymbol{X}_k^T, \boldsymbol{\Theta}_k^T\right)^T \in \mathbb{R}^{n_x}$, with $(\cdot)^T$ being the transpose operator, is the unknown system state vector at time step $k$, $k = 1, 2, ..., K$, where $K$ is the maximum number of time steps. The vector $\boldsymbol{x}_k$ consists of the object kinematic state vector $\boldsymbol{X}_k$ and object extent, characterised by the parameter vector $\boldsymbol{\Theta}_k \in \mathbb{R}^{n_\Theta}$; $f(\cdot)$ and $h(\cdot)$ are respectively the system and the measurement functions, nonlinear in general; $\boldsymbol{z}_k \in \mathbb{R}^{n_z}$ is the measurement vector and $\boldsymbol{\eta}_k = (\boldsymbol{\eta}_{s,k}^T \ \boldsymbol{\eta}_{p,k}^T)^T$ and $\boldsymbol{w}_k$ are the system (kinematic state and parameters) and measurement noises, respectively.

Within the SMC approach the system state pdf is approximated by randomly generated samples and based on the sequence of measurements. According to the Bayes' rule the filtering pdf $p(\boldsymbol{x}_k|\boldsymbol{z}_{1:k})$ of the state vector $\boldsymbol{x}_k$ given a sequence of sensor measurements $\boldsymbol{z}_{1:k}$ up to time $k$ can be written as

$$p(\boldsymbol{x}_k|\boldsymbol{z}_{1:k}) = \frac{p(\boldsymbol{z}_k|\boldsymbol{x}_k)p(\boldsymbol{x}_k|\boldsymbol{z}_{1:k-1})}{p(\boldsymbol{z}_k|\boldsymbol{z}_{1:k-1})}, \tag{3}$$

where $p(\boldsymbol{z}_k|\boldsymbol{z}_{1:k-1})$ is a normalising constant. The state *predictive* distribution is given by the equation

$$p(\boldsymbol{x}_k|\boldsymbol{z}_{1:k-1}) = \int_{\mathbb{R}^{n_x}} p(\boldsymbol{x}_k|\boldsymbol{x}_{k-1})p(\boldsymbol{x}_{k-1}|\boldsymbol{z}_{1:k-1})d\boldsymbol{x}_{k-1}. \tag{4}$$

The evaluation of the right hand side of (3) involves integration which can be performed by the PF approach [2] by approximating the posterior pdf $p(\boldsymbol{x}_k|\boldsymbol{z}_{1:k})$ with a set of particles $\boldsymbol{x}_{0:k}^{(i)}$, $i = 1, \ldots, N$ and their corresponding weights $w_k^{(i)}$. Then the posterior density function can be written as follows

$$p(\boldsymbol{x}_{0:k}|\boldsymbol{z}_{1:k}) = \sum_{i=1}^{N} w_k^{(i)} \delta(\boldsymbol{x}_{0:k} - \boldsymbol{x}_{0:k}^{(i)}), \tag{5}$$

where $\delta(.)$ is the Dirac delta function, and the weights are normalised such that $\sum_i w_k^{(i)} = 1$.

Each pair $\{\boldsymbol{x}_{0:k}^{(i)}, w_k^{(i)}\}$ characterises the belief that the object is in state $\boldsymbol{x}_{0:k}^{(i)}$. An estimate of the variable of interest is obtained by the weighted sum of particles. Two major stages can be distinguished: *prediction* and *update*. During prediction, each particle is modified according to the state model, including the addition of random noise in order to simulate the effect of the noise on the state. In the update stage, each particle's weight is re-evaluated based on the new data. A *resampling* procedure introduces variety in the particles by eliminating those with small weights and replicating the particles with larger weights such that the approximation in (5) still holds. The residual resampling algorithm [8] is applied here.

## III. Measurement Likelihood for the Extended Object Derived Based on Border Parameterisation

In the context of extended object tracking, the prediction step is generally well studied for various classes of interval and spatial representations of uncertainties. Ellipsoids, spheres and polytope families can be easily propagated when the system dynamics and sensor models are linear. In case of nonlinear models, other alternatives are the interval analysis methods using boxes [24].

The update step with the likelihood calculation is less studied or often studied with a restriction to a particular class of sets of a particular type of measurements. The aim of this paper is to derive general likelihood calculation procedures based on Monte Carlo methods without a restriction on the type of a set of interest or the type of measurement available. For that purpose, the main idea of this paper is to introduce a sampling step for regions of interest in the extended object. This sampling aims to represent the probability of a given point, in the state space, to be the origin of a measurement. This section describes in detail the newly proposed method. As an illustration, the case of an extended object with circular form is considered.

Without loss of generality, assume that there is only one static sensor described by its state vector $\boldsymbol{x}_{s,k}$. Assume that at each measurement time $k$ the extended object generates a matrix $\boldsymbol{Z}_k = \{\boldsymbol{z}_k^1, \ldots, \boldsymbol{z}_k^m\} \in \mathbb{R}^{n_z \times M_k}$ of $M_k$

measurement vectors. The number of measurements $M_k$ originating from the visible border of the source is considered Poisson-distributed random variable with mean value of $\lambda$, i.e. $M_k \sim Poisson(\lambda)$. The measurements originating from a target are assumed to be conditionally independent, i.e.

$$p(\boldsymbol{Z}_k|\boldsymbol{x}_k) = \prod_{j=1}^{M_k} p(\boldsymbol{z}_k^j|\boldsymbol{x}_k). \quad (6)$$

If at time step $k-1$ the posterior pdf $p(\boldsymbol{x}_{k-1}|\boldsymbol{z}_{k-1}^j)$ is known, then one can express the prior $p(\boldsymbol{x}_k|\boldsymbol{z}_{k-1}^j)$ via the Chapman-Kolmogorov equation:

$$p(\boldsymbol{x}_k|\boldsymbol{z}_{k-1}^j) = \int_{\mathbb{R}^{n_x}} p(\boldsymbol{x}_k|\boldsymbol{x}_{k-1}) p(\boldsymbol{x}_{k-1}|\boldsymbol{z}_{k-1}^j) d\boldsymbol{x}_{k-1}. \quad (7)$$

### A. Model of the Extended Targets

The nearly constant velocity model [33], [34] is used to model the motion of the centre of the region surrounding the extended target. In two dimensions, the state of the target is given by:

$$\boldsymbol{X}_k = \boldsymbol{A}\boldsymbol{X}_{k-1} + \boldsymbol{\Gamma}\boldsymbol{\eta}_{s,k-1}, \quad (8)$$

where $\boldsymbol{X}_k = (x_{c,k}, \dot{x}_{c,k}, y_{c,k}, \dot{y}_{c,k})^T$ is a vector containing the position coordinates and velocity of the center of the extent; $\boldsymbol{A} = diag(\boldsymbol{A}_1, \boldsymbol{A}_1)$, $\boldsymbol{A}_1 = \begin{pmatrix} 1 & T_s \\ 0 & 1 \end{pmatrix}$, $\boldsymbol{\Gamma} = \begin{pmatrix} T_s^2/2 & T_s & 0 & 0 \\ 0 & 0 & T_s^2/2 & T_s \end{pmatrix}^T$, $T_s$ is the sampling interval and $\boldsymbol{\eta}_{s,k-1} = (\sigma_x \ \ \sigma_y)^T$ is the standard deviation of the system dynamics noise. Then the system dynamics noise is represented as a Gaussian noise process with covariance $\boldsymbol{Q} = diag(\boldsymbol{Q}_1\sigma_x^2, \boldsymbol{Q}_1\sigma_y^2)$, where $\boldsymbol{Q}_1 = \begin{pmatrix} T_s^4/4 & T_s^3/2 \\ T_s^3/2 & T_s^2 \end{pmatrix}$. The evolution model for the extent is assumed to be

$$\boldsymbol{\Theta}_k = \boldsymbol{\Theta}_{k-1} + \boldsymbol{\eta}_{p,k-1}. \quad (9)$$

Then again, the augmented state vector is $\boldsymbol{x}_k = (\boldsymbol{X}_k^T, \boldsymbol{\Theta}_k^T)^T$.

### B. Observation Model

Range and bearing observations from a network of low cost sensors positioned along the road are considered as measurements. The measurement vector is $\boldsymbol{z}_k^j = (d_k^j, \beta_k^j)^T$, where $d_k^j$ is the range and $\beta_k^j$ is the bearing of the measurement point $j$. The measurement equation is of the form:

$$\boldsymbol{z}_k^j = h(\boldsymbol{x}_k) + \boldsymbol{w}_k^j, \quad (10)$$

where $h$ is the nonlinear function

$$h(\boldsymbol{x}_k) = \left( \sqrt{x_k^{j2} + y_k^{j2}}, \tan^{-1}\frac{y_k^j}{x_k^j} \right), \quad (11)$$

$x_k^j$ and $y_k^j$ denote the Cartesian coordinates of the actual point of the source from where the measurement emanates in the case of two dimensional space. The measurement noise $\boldsymbol{w}_k^j$ is supposed to be Gaussian, with a known covariance matrix $\boldsymbol{R} = diag(\sigma_d^2, \sigma_\beta^2)$. That contains the components for the range and for the bearing.

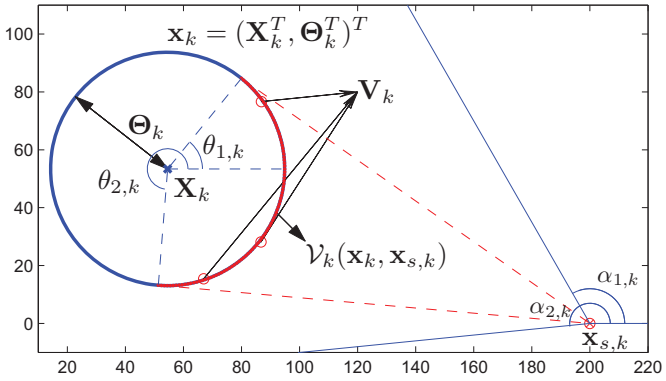


Figure 1. Notations and definitions in the context of *Example 1*

### C. Introduction of the Notion of the Visible Surface

Next, the measurement likelihood $p(\boldsymbol{z}_k^j|\boldsymbol{x}_k)$ of the extended target can be represented with the relation

$$p(\boldsymbol{z}_k^j|\boldsymbol{x}_k) = \int_{\mathbb{R}^{n_v}} p(\boldsymbol{z}_k^j|\boldsymbol{V}_k) p(\boldsymbol{V}_k|\boldsymbol{x}_k) d\boldsymbol{V}_k, \quad (12)$$

where $\boldsymbol{V}_k \in \mathbb{R}^{n_v}$ denotes a source of measurement in the state space. In practice, these visible sources $\boldsymbol{V}_k$ depend on the object position, nature and parameters $\boldsymbol{x}_k$ and on the sensor state (e.g., the sensor position and angle of view). The pdf $p(\boldsymbol{V}_k|\boldsymbol{x}_k)$ represents the probability of a point in the state space to be a source of measurement given the extended object $\boldsymbol{x}_k$. The surface of the target with state $\boldsymbol{x}_k$ visible from the sensor with state $\boldsymbol{x}_{s,k}$ is denoted by $\mathcal{V}_k(\boldsymbol{x}_k, \boldsymbol{x}_{s,k})$.

We assume that the sources of the measurements at time step $k$, given the target state and the sensor prior state are uniformly distributed along the region $\mathcal{V}_k(\boldsymbol{x}_k, \boldsymbol{x}_{s,k})$, visible from the sensor $\boldsymbol{x}_{s,k}$, i.e.

$$p(\boldsymbol{V}_k|\boldsymbol{x}_k) = p(\boldsymbol{V}_k|\boldsymbol{x}_k, \boldsymbol{x}_{s,k}) = \mathcal{U}_{\mathcal{V}_k(\boldsymbol{x}_k, \boldsymbol{x}_{s,k})}(\boldsymbol{V}_k), \quad (13)$$

where $\mathcal{U}_{\mathcal{V}_k(\boldsymbol{x}_k, \boldsymbol{x}_{s,k})}(\cdot)$ represents the uniform pdf with the support $\mathcal{V}_k(\boldsymbol{x}_k, \boldsymbol{x}_{s,k})$.

Inserting (13) into (12) gives

$$p(\boldsymbol{z}_k^j|\boldsymbol{x}_k) = \int_{\mathbb{R}^{n_v}} p(\boldsymbol{z}_k^j|\boldsymbol{V}_k) \mathcal{U}_{\mathcal{V}_k(\boldsymbol{x}_k, \boldsymbol{x}_{s,k})}(\boldsymbol{V}_k) d\boldsymbol{V}_k = \\ = \frac{1}{||\mathcal{V}_k(\boldsymbol{x}_k, \boldsymbol{x}_{s,k})||} \int_{\mathcal{V}_k(\boldsymbol{x}_k, \boldsymbol{x}_{s,k})} p(\boldsymbol{z}_k^j|\boldsymbol{V}_k) d\boldsymbol{V}_k, \quad (14)$$

where $||\mathcal{V}_k(\boldsymbol{x}_k, \boldsymbol{x}_{s,k})||$ denotes some measure of the region $\mathcal{V}_k(\boldsymbol{x}_k, \boldsymbol{x}_{s,k})$. This measure represents the length of a curve (a one-dimensional concept), the area of a surface (a two-dimensional concept) or the volume of a solid (a three-dimensional topological manifold). Unfortunately, as it is shown in *Example 1*, the integral in (14) is not simple to calculate.

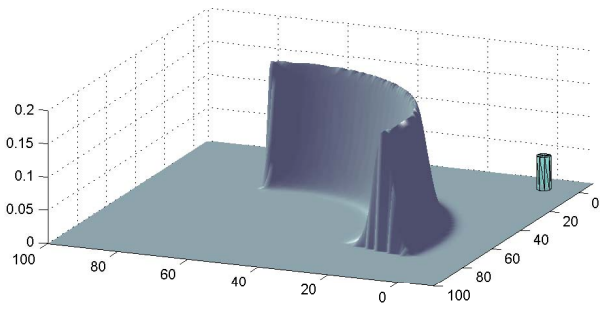


Figure 2. Illustrative visualisation of the likelihood function in the context of *Example 1*

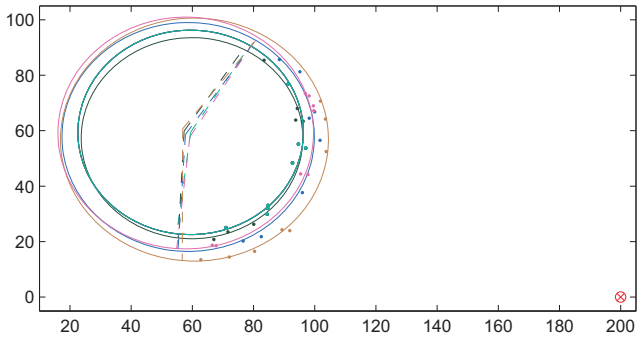


Figure 3. Sampling $S = 8$ samples $\left\{\widetilde{\boldsymbol{V}}_k^{(i,\ell)}\right\}_{l=1}^{S}$ based on (19) for each of $i = 1, ..., N$ extended object particles, where $N = 5$

*Example 1:* Consider a two dimensional problem with an extended object of a circular form as shown in Figure 1. The parameter $\boldsymbol{\Theta}_k = r_k$ represents the radius of the circle of the extent. Assume that one measurement is constituted of range and bearing available at each time step and that the likelihood function $p(\boldsymbol{z}_k^j|\boldsymbol{V}_k)$ is equal to the Gaussian distribution, i.e., $\mathcal{N}(\boldsymbol{z}_k^j; h(\boldsymbol{V}_k), \boldsymbol{R})$. Therefore, using (14), the likelihood function can be expressed as

$$p(\boldsymbol{z}_k^j|\boldsymbol{x}_k) = \frac{1}{||\mathcal{V}_k(\boldsymbol{x}_k, \boldsymbol{x}_{s,k})||} \int\limits_{\mathcal{V}_k(\boldsymbol{x}_k, \boldsymbol{x}_{s,k})} \mathcal{N}(\boldsymbol{z}_k^j; h(\boldsymbol{V}_k), \boldsymbol{R}) d\boldsymbol{V}_k. \tag{15}$$

Visual interpretation of (15) is shown in Figure 2. The prior sensor state is given by $\boldsymbol{x}_{s,k} = (x_{s,k}, y_{s,k}, \alpha_{1,k}, \alpha_{2,k})^T$, where $(x_{s,k}, y_{s,k})$ are the sensor position coordinates, $\alpha_{1,k}$ and $\alpha_{2,k}$ represent two parameters defining the angle of view of the sensor. At each time step $k$, if the extended target is visible from the sensor, then the two angles $\alpha_{1,k}$ and $\alpha_{2,k}$ define geometrically other two angles $\theta_{1,k}$, $\theta_{2,k}$ that specify the visible border $\mathcal{V}_k(\boldsymbol{x}_k, \boldsymbol{x}_{s,k})$, i.e.

$$\mathcal{V}_k(\boldsymbol{x}_k, \boldsymbol{x}_{s,k}) = \{(x_{c,k} + r_k \cos(\theta_k), y_{c,k} + r_k \sin(\theta_k))\}, \tag{16}$$

where $\theta_k \in [\theta_{1,k}, \theta_{2,k}]$. Substituting (16) into (14) gives the likelihood function

$$p(\boldsymbol{z}_k^j|\boldsymbol{x}_k) = \frac{1}{\sqrt{2\pi|\boldsymbol{R}|}\ ||\mathcal{V}_k(\boldsymbol{x}_k, \boldsymbol{x}_{s,k})||} \int\limits_{\theta_{1,k}}^{\theta_{2,k}} e^{-\frac{(\boldsymbol{z}_k^j - \boldsymbol{z}_k^{\theta_k})\boldsymbol{R}^{-1}(\boldsymbol{z}_k^j - \boldsymbol{z}_k^{\theta_k})^T}{2}} d\theta_k, \tag{17}$$

where $\boldsymbol{z}_k^\theta \triangleq \tan^{-1}\left(\frac{y_{c,k} + r_k \sin(\theta_k) - y_{s,k}}{x_{c,k} + r_k \cos(\theta_k) - x_{s,k}}\right)$ is the measurement predicted by the filter. The measurement sources are generated uniformly distributed on the border of the visible object as seen from the sensor. The measurement noise in the bearing and the range are assumed to be with Gaussian distribution. To the best of our knowledge, unfortunately there is no analytic solution to this integral. In the next Section, a Monte Carlo method is described capable of approximating $p(\boldsymbol{z}_k^j|\boldsymbol{x}_k)$. ■

### D. Parametrisation of the Visible Border $\mathcal{V}_k(\boldsymbol{x}_k, \boldsymbol{x}_{s,k})$

The calculation of the likelihood (12) can be performed using a Monte Carlo method in the following way:

First, the visible border $\mathcal{V}_k(\boldsymbol{x}_{k|k-1}^{(i)}, \boldsymbol{x}_{s,k})$ is determined. The aim is to sample from a set of $S$ visible points $\{\boldsymbol{V}_k^{(i,\ell)}\}_{\ell=1}^{S}$ from the likelihood function $p(\boldsymbol{V}_k^{(i)}|\boldsymbol{x}_k)$, for each particle $i$. After the prediction step, a set of weighted particles $\{(\boldsymbol{x}_{k|k-1}^{(i)}, w_{k|k-1}^{(i)})\}_{i=1}^{N}$ is available (recall that each of the $N$ particles can be seen as an extended object hypothesis). This sampling process can be performed differently. Two ways are presented in the following *Example 2* with uniform distribution over the visible angular interval and based on the angular measurements, with added Gaussian noise in both cases.

*Example 2:* Consider the same problem as in Example 1.

i) For each particle $\boldsymbol{x}_{k|k-1}^{(i)}$ the support of $p(\boldsymbol{V}_k|\boldsymbol{x}_{k|k-1}^{(i)})$ can be defined by uniform distribution over $\mathcal{V}_k(\boldsymbol{x}_{k|k-1}^{(i)}, \boldsymbol{x}_{s,k})$. From equation (16), a source $\boldsymbol{V}_k \in \mathcal{V}_k(\boldsymbol{x}_{k|k-1}^{(i)}, \boldsymbol{x}_{s,k})$ can be characterised by

$$\boldsymbol{V}_k^{(i)} = \begin{pmatrix} r_{v,k}^{(i)} \\ \theta_{v,k}^{(i)} \end{pmatrix}, \tag{18}$$

where $r_{v,k}^{(i)}$ and $\theta_{v,k}^{(i)}$ are respectively noisy radius and angle samples. A Gaussian distribution with mean the radius of the extent and standard deviation $\tilde{\sigma}_r$ is chosen for the radius noise. For the angle a uniform pdf over $[\theta_{1,k}, \theta_{2,k}]$ is chosen, i.e.:

$$p(\boldsymbol{V}_k|\boldsymbol{x}_{k|k-1}^{(i)}) = \begin{pmatrix} \mathcal{N}(r_{v,k}^{(i)}; r_k^{(i)}, \tilde{\sigma}_r^2) \\ \mathcal{U}_{[\theta_{1,k}, \theta_{2,k}]}(\theta_{v,k}^{(i)}) \end{pmatrix}. \tag{19}$$

Example of sampling based on (19) is shown in Figure 3.

ii) Having a measurement $\boldsymbol{z}_k^j$, instead of sampling by (19) one can sample from $p(\boldsymbol{V}_k|\boldsymbol{x}_{k|k-1}^{(i)}, \boldsymbol{z}_k^j)$:

$$p(\boldsymbol{V}_k|\boldsymbol{x}_{k|k-1}^{(i)}) = \begin{pmatrix} \mathcal{N}(r_{v,k}^{(i)}; r_k^{(i)}, \tilde{\sigma}_r^2) \\ \mathcal{N}(\theta_{v,k}^{(i)}; \theta_k^{(i,j)}, \tilde{\sigma}_\theta{}^2) \end{pmatrix}, \tag{20}$$

where $\theta_k^{(i,j)}$ is an angle depending of the $j^{th}$ bearing measurement and the $i^{th}$ particle extent and $\tilde{\sigma}_\theta$ is the standard

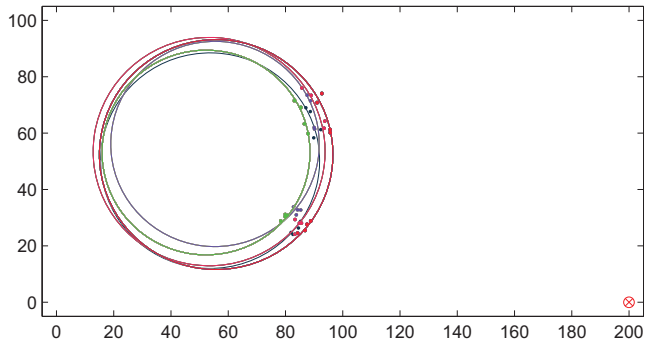


Figure 4. Sampling $Q = 2$ samples per measurement $\left\{\widetilde{\boldsymbol{V}}_k^{(i,q)}\right\}_{q=1}^{Q}$ based on (20) for $M_k = 4$ measurements, which leads to a total of 8 samples drawn for each of $N = 5$ extended object particles

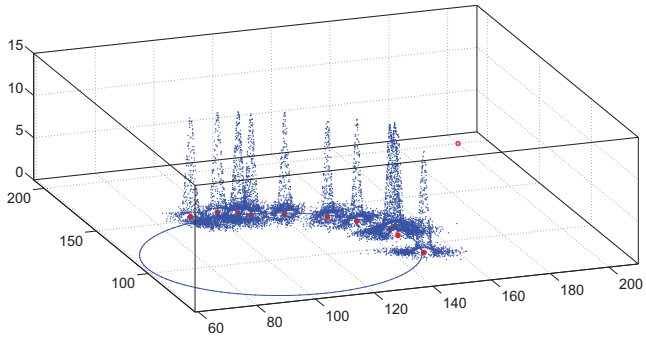


Figure 5. Parametrisation of the likelihood function in the context of *Example 2* for samples based on the measurement angular direction (generated using equations (20) and (21) )

deviation for the angle used for generating the samples. Note that for $N$ particles and $Q$ samples from the visible region per each of $M_k$ measurements we have a total of $NQM_k$ samples. Example of sampling based on (20) is shown in Figure 4. Visualisation of sampling based on measurement angular direction information is presented in Figure 5. ■

Once the points $\{\widetilde{\boldsymbol{V}}_k^{(i,\ell)}\}_{\ell=1}^{S}$ are available for each particle $\boldsymbol{x}_{k|k-1}^{(i)}$, we can approximate the likelihood (see the equation (12)) according to

$$p(\boldsymbol{z}_k^j|\boldsymbol{x}_{k|k-1}^{(i)}) = \int_{\mathbb{R}^{n_x}} p(\boldsymbol{z}_k^j|\boldsymbol{V}_k)p(\boldsymbol{V}_k, \boldsymbol{x}_{k|k-1}^{(i)})d\boldsymbol{V}_k,$$

$$= \sum_{\ell=1}^{M_k} w_{k|k-1}^{(i)} p(\boldsymbol{z}_k^j|\widetilde{\boldsymbol{V}}_k^{(i,\ell)})p(\widetilde{\boldsymbol{V}}_k^{(i,\ell)}|\boldsymbol{x}_{k|k-1}^{(i)}). \tag{21}$$

The term $p(\boldsymbol{z}_k^j|\widetilde{\boldsymbol{V}}_k^{(i,\ell)})$ in (21) can be easily calculated in a classical way depending on the problem, for example using a Gaussian measurement noise distribution

$$p(\boldsymbol{z}_k^j|\widetilde{\boldsymbol{V}}_k^{(i,\ell)}) = \frac{1}{\sqrt{2\pi||\boldsymbol{R}||}} e^{-\frac{(\boldsymbol{z}_k^j - \boldsymbol{z}_k^{(i,\ell)})\boldsymbol{R}^{-1}(\boldsymbol{z}_k^j - \boldsymbol{z}_k^{(i,\ell)})^T}{2}}. \tag{22}$$

The term $p(\widetilde{\boldsymbol{V}}_k^{(i,\ell)}|\boldsymbol{x}_{k|k-1}^{(i)})$ depends very much on the visible set $\mathcal{V}_k(\boldsymbol{x}_{k|k-1}^{(i)}, \boldsymbol{x}_{s,k})$. It can be seen as

$$p(\widetilde{\boldsymbol{V}}_k^{(i,\ell)}|\boldsymbol{x}_{k|k-1}^{(i)}) = p(\widetilde{\boldsymbol{V}}_k^{(i,\ell)} \in \mathcal{V}_k(\boldsymbol{x}_{k|k-1}^{(i)}, \boldsymbol{x}_{s,k})). \tag{23}$$

Let us illustrate the calculation of the term $p(\widetilde{\boldsymbol{V}}_k^{(i,\ell)}|\boldsymbol{x}_{k|k-1}^{(i)})$ over the circle using the same problem as in Example 1.

*Example 3:* Consider the same problem as in the previous examples. Let us denote with $x_{v,k}^{(i,\ell)}$ and $y_{v,k}^{(i,\ell)}$ the coordinates of $\widetilde{\boldsymbol{V}}_k^{(i,\ell)}$, i.e. $\widetilde{\boldsymbol{V}}_k^{(i,\ell)} = (x_{v,k}^{(i,\ell)}, y_{v,k}^{(i,\ell)})^T$. Recall that according to (16) the border $\mathcal{V}_k(\boldsymbol{x}_{k|k-1}^{(i)}, \boldsymbol{x}_{s,k})$ can be written as

$$\mathcal{V}_k(\boldsymbol{x}_{k|k-1}^{(i)}, \boldsymbol{x}_{s,k}) = \{(x_{c,k|k-1}^{(i)} + r_{k|k-1}^{(i)}\cos(\theta_k), \tag{24}$$
$$y_{c,k|k-1}^{(i)} + r_{k|k-1}^{(i)}\sin(\theta_k)), \theta_k \in [\theta_{1,k|k-1}^{(i)}, \theta_{2,k|k-1}^{(i)}]\}.$$

A simple expression of $p(\widetilde{\boldsymbol{V}}_k^{(i,\ell)}|\boldsymbol{x}_{k|k-1}^{(i)})$ can be

$$p(\widetilde{\boldsymbol{V}}_k^{(i,\ell)}|\boldsymbol{x}_{k|k-1}^{(i)}) = \mathcal{L}_k^{\theta,(i)}\mathcal{L}_k^{r,(i)} \tag{25}$$

with

$$\mathcal{L}_k^{\theta,(i)} = \tag{26}$$
$$I_{[\theta_{1,k|k-1}^{(i)}-\epsilon, \theta_{2k|k-1}^{(i)}+\epsilon]}\left(\tan^{-1}\left(\frac{y_{v,k}^{(i,\ell)} - y_{c,k}^{(i)}}{x_{v,k}^{(i,\ell)} - x_{c,k}^{(i)}}\right)\right)$$

and

$$\mathcal{L}_k^{r,(i)} = \tag{27}$$
$$\mathcal{N}(\sqrt{(x_{v,k}^{(i,\ell)} - x_{c,k}^{(i)})^2 + (y_{v,k}^{(i,\ell)} - y_{c,k}^{(i)})^2}, r_{k|k-1}^{(i)}, \sigma_r^2),$$

where $I_{[\theta_{1,k|k-1}^{(i)}-\epsilon, \theta_{2k|k-1}^{(i)}+\epsilon]}$ is the indicator function over the interval $[\theta_{1,k|k-1}^{(i)}-\epsilon, \theta_{2k|k-1}^{(i)}+\epsilon]$, $\epsilon$ is a positive real number to parameterise a larger angle of view while $\sigma_r$ is the standard deviation for a Gaussian likelihood applied to the distance from $\widetilde{\boldsymbol{V}}_k^{(i,\ell)}$ to the center of the particle $(x_{c,k}^{(i)}, y_{c,k}^{(i)})$.

Visual representation for the visible border parametrisation of *Example 3* can be seen in Figure 6. ■

In the following section the case of measurements consisting of range and bearing is studied.

## IV. A Particle Filter for Extended Object Tracking

Based on the algorithmic approach described in the previous two sections a particle filter is implemented for extended object tracking. The filter implementation is given in Table I.

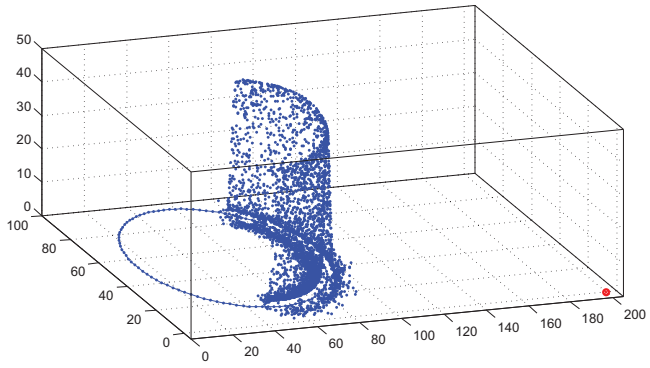

Figure 6. Likelihood function based on equation (25)

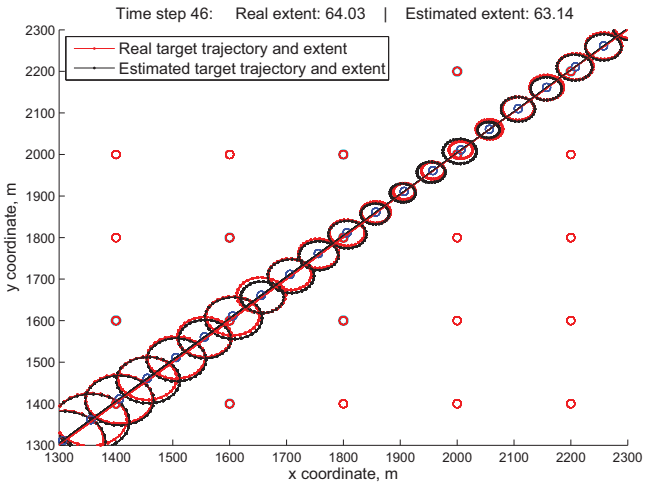


Figure 7. Actual and estimated position and actual and estimated extent from one run for the simulation scenario with $N = 80$ extended object particles and $H = 5$ Metropolis-Hastings iterations. For the actual object the direction of extension/shrinkage is retained with 95% probability, i.e. if the object is currently extending there is 5% probability that it will start shrinking on the next time step. The fluctuation of the radius of the extent is limited between $10\,m$ and $110\,m$. These fluctuations are unknown for the filter.

**Table I. A particle filter for extended object tracking**

*Initialisation*

I. $k = 0$, for $i = 1, \ldots, N$, generate particles $\{\boldsymbol{x}_0^{(i)} \sim p(\boldsymbol{x}_0)\}$, where the initial particle weights are $\{w_0^{(i)}\}_{i=1}^N = 1/N$.

II. Repeat steps 1) to 6) for $k = 1, 2, \ldots, K$:

1) *Prediction Step*
For $i = 1, \ldots, N$, generate samples $\boldsymbol{x}_k^{(i)}$ from (8).

2) *Measurement Update*
On the receipt of a new measurement evaluate the importance weights for $i = 1, \ldots, N$,

$$w_{k|k-1}^{(i)} = w_{k-1}^{(i)} p(\boldsymbol{z}_k^j | \boldsymbol{x}_{k|k-1}^{(i)}). \tag{28}$$

The likelihood $p(\boldsymbol{z}_k^j | \boldsymbol{x}_{k|k-1}^{(i)})$ is calculated after generating $M_k$ samples from the visible border $\{\boldsymbol{V}_k^{(j)}\}_{j=1}^{M_k}$, and substituting (25), (26) and (27) into (21).

3) *Output*
The estimation can be calculated as the posterior mean $E[\boldsymbol{x}_k | \boldsymbol{z}_{1:k}]$, or by weighting the particles

$$\hat{\boldsymbol{x}}_k = E[\boldsymbol{x}_k | \boldsymbol{z}_{1:k}] = \sum_{i=1}^{N} \hat{w}_{k|k-1}^{(i)} \boldsymbol{x}_k^{(i)}. \tag{29}$$

4) *Computing the effective sample size*
$N_{eff} = 1/\sum_{i=1}^{N} (\hat{w}_{k|k-1}^{(i)})^2$, choosen threshold, for example $N_{thresh} = 2N/3$.

5) *Selection step (resampling)*
If $N_{eff} < N_{thresh}$ perform Sequential Importance Resampling (SIR); for $i = 1, \ldots, N$, set $w_{k|k-1}^{(i)} = \hat{w}_{k|k-1}^{(i)} = 1/N$.

A better choice for the extended object particles can be made employing the Metropolis-Hastings (MH) algorithm described in Table II, instead of steps 1) and 2) from the algorithm in Table I.

**Table II. Metropolis-Hastings approach for choosing appropriate extended object hypotheses**

Repeat for $h = 1, ..., H$, where $H$ is the number of Metropolis-Hastings iteration steps:

1) *Proposing particles*
For each extended object hypothesis $\{\boldsymbol{x}_{k|k-1}^{(i)}\}_{i=1}^N$ generate a proposal particle $\{\boldsymbol{x}_{k|k-1}^{(i)(h)}\}_{i=1}^N$, then sample $\{\widetilde{\boldsymbol{V}}_k^{(i,\ell)}\}_{\ell=1}^S$ for that proposal.

2) *Accepting particles*
Repeat for $i = 1, ..., N$:
Initialise $\boldsymbol{x}_{k|k-1}^{(i)} = \boldsymbol{x}_{k|k-1}^{(i)(1)}$. On receipt of new measurements evaluate the likelihood function of the proposal for the current extended hypothesis using (25). From the likelihood functions ratio according to the Metropolis-Hastings's rule:

$$\boldsymbol{x}_{k|k-1}^{(i)} = \begin{cases} \boldsymbol{x}_{k|k-1}^{(i)(h)} & \min\left(1, \frac{p(\boldsymbol{Z}_k | \boldsymbol{x}_{k|k-1}^{(i)(h)})}{p(\boldsymbol{Z}_k | \boldsymbol{x}_{k|k-1}^{(i)})}\right) \\ \text{(reject)} & \text{otherwise.} \end{cases}$$

## V. Performance Evaluation

Simulations are performed for 100 time steps each repeated for 200 iterations in the case of tracking of object with circular extent and measurements consisting of range and bearing.

Several scenarios are simulated with an increasing number of extended object particles from 50 to 300. For each of these particles 5 Metropolis-Hastings proposals are generated. The initial position of the object is biased by Gaussian random noise of 10 $m$ for both coordinates. The initial extent is altered by Gaussian noise with standard deviation of 5 $m$ in radius, and the initial velocity is generated with added Gaussian noise with standard deviation of 0.5 $m/s$ for each of the coordinates.

The number of measurements generated in each step is Poisson distributed, i.e. $M_k \sim Poisson(\lambda)$, where $\lambda = 5$. For each measurement and each hypothesis one random sample $Q$ is generated according to (20). The standard deviations for the bearing and for the radius of these samples are respectively $\sigma_\beta = 3^\circ$ and $\sigma_r = 1\,m$. The sensor line of sight for simplicity is determined by the following angles $\alpha_{1,k} = 0$ and $\alpha_{2,k} = 2\pi$.

The measurements are assumed to originate from random locations of the visible frontier of the extent where the angular position is uniformly distributed over the visible arc and the range has additive random Gaussian noise with standard deviation of $2\,m$. They are generated in a similar manner to the sampling described in (19).

The change of the size of the extent in the space-state evolution model is generated by adding/substracting (corresponding to extension/shrinkage) the absolute value of a Gaussian random variable with zero mean and standard deviation $2\,m$. The actual target trajectory is generated based on (1) with noise covariance equal to zero. The change of the size of the extent when generating the extended object particles is modeled a random walk using normally distributed random variable with zero mean and standard deviation $4\,m$. The trajectory prediction in the filter is performed with standard deviation for the components of the system dynamic noise $\sigma_x = 0.5\,m/s^2$ and $\sigma_y = 0.5\,m/s^2$, respectively.

Graph results are presented in Figures 7 through 10. Figure 7 presents the trajectory of a scenario with $N = 80$ extended object particles and 5 Metropolis-Hastings iterations. Also, on that figure the sensor network can be seen that uses only one active sensor at a time. Figures 8, 9 and 10 plot the results for position, extent and velocity with a different number of particles. Tabular results for the success rate and for the computational time per time step are shown in Table III. A target is considered lost (and the current iteration failed) when the likelihood function (25) has value lower than $10^{-6}$ for five consecutive steps. The presented results show the effectiveness of the algorithm.

## VI. Conclusions

This paper develops a novel SMC approach for extended object tracking based on nonlinear measurements and border parametrisation. A key challenge for extended object tracking is the presence of multiple measurements. To cope with the extended object tracking problem we derive an expression for the likelihood function. This likelihood function is calculated using SMC integration. An example with a circular extended object is given. The simulation results demonstrate the effectiveness of the proposed solution. Based on the proposed

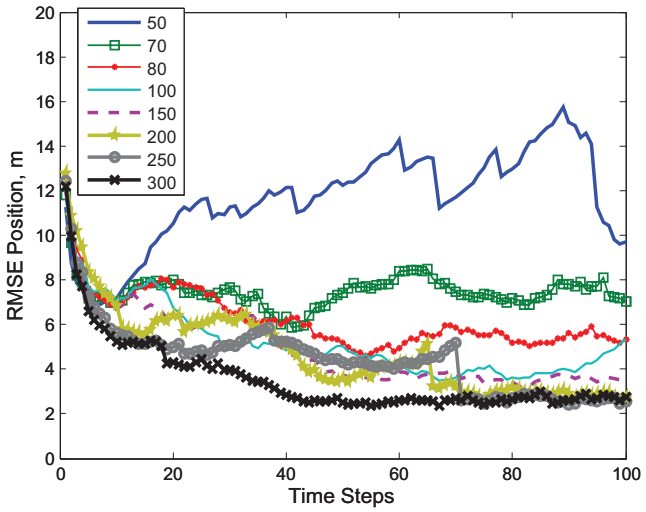


Figure 8. Comparison of the results for the RMSE of the position for 200 iterations and number of particles from 50 to 300

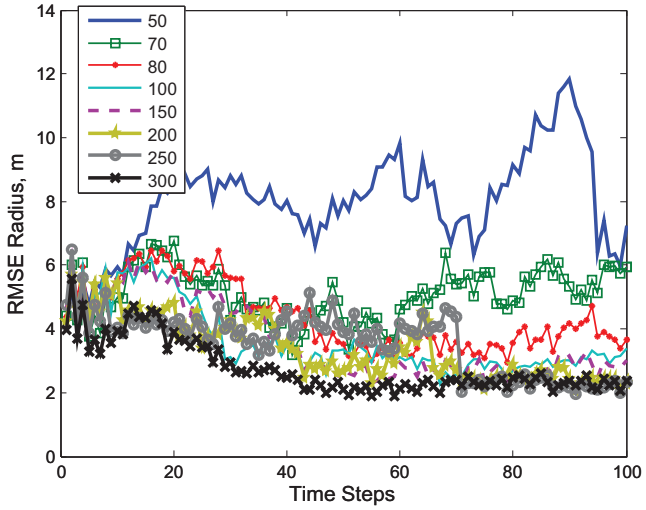


Figure 9. Results for the RMSE of the radius for 200 iterations and number of particles from 50 to 300

Table III
Computational time and Success rate for 200 iterations and varying number of $M_k \sim Poisson(5)$ measurements

| $N$ particles (total average of $NM_kQ$ samples) | Success rate, % | Computational time, sec |
|---|---|---|
| 50 (250) | 0.945 | 0.606 |
| 70 (350) | 0.995 | 0.938 |
| 80 (400) | 1.000 | 1.055 |
| 100 (500) | 0.99 | 1.401 |
| 150 (750) | 1.000 | 2.123 |
| 200 (1000) | 0.985 | 2.843 |
| 250 (1250) | 0.995 | 3.981 |
| 300 (1500) | 1.000 | 4.846 |

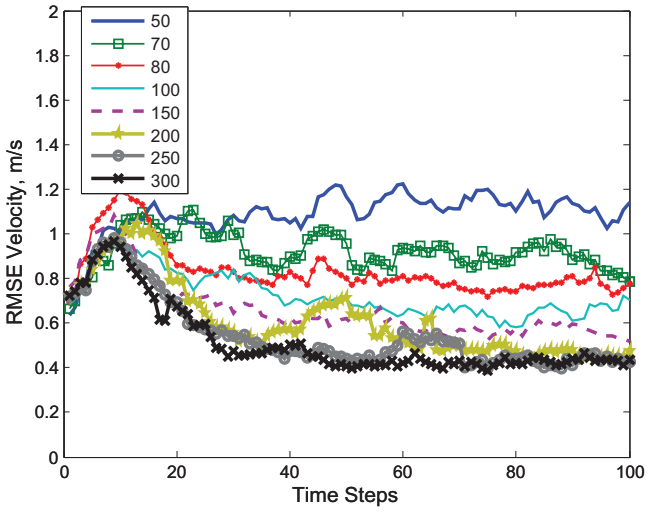


Figure 10. Comparison of the results for the RMSE of the velocity for number of particles from 50 to 300

approach future work will be focused on studies with more complex target shape, such as ellipsoids and measurements originating from group objects.

## VII. Acknowledgments

We acknowledge the support from the [European Community's] Seventh Framework Programme [FP7/2007-2013] under grant agreement No 238710 (Monte Carlo based Innovative Management and Processing for an Unrivalled Leap in Sensor Exploitation), the EU COST action TU0702 and the Bulgarian National Science Fund, grant DTK 02/28/2009.

## References

[1] A. Doucet, N. Freitas, and E. N. Gordon, *Sequential Monte Carlo Methods in Practice*. New York: Springer-Verlag, 2001.

[2] M. Arulampalam, S. Maskell, N. Gordon, and T. Clapp, "A tutorial on particle filters for online nonlinear/non-Gaussian Bayesian tracking," *IEEE Trans. on Signal Proc.*, vol. 50, no. 2, pp. 174–188, 2002.

[3] F. Gustafsson, "Particle filter theory and practice with positioning applications," *IEEE Transactions on Aerospace and Electronics Systems Magazine Part II: Tutorials*, vol. 25, no. 7, pp. 53–82, 2010.

[4] A. Jaswinski, *Stochastic Processes and Filtering Theory*. New York: Academic Press, 1970.

[5] S. Julier, J. Uhlmann, and H. Durrant-White, "A new approach for filtering nonlinear systems," in *Proc. of the Amer. Control Conf.*, Washington, DC, 1995.

[6] S. Julier and J. Uhlmann, "Unscented filtering and nonlinear estimation," *Proceedings of the IEEE*, vol. 92, no. 3, pp. 401–422, 2004.

[7] S. Julier, "The scaled unscented transformation," in *Proc. IEEE American Control Conf.*, 2002, pp. 4555–4559.

[8] E. Wan and R. van der Merwe, *The Unscented Kalman Filter, Ch. 7: Kalman Filtering and Neural Networks. Edited by S. Haykin*. Wiley Publishing, September 2001, pp. 221–280.

[9] B. Ristic, S. Arulampalam, and N. Gordon, *Beyond the Kalman Filter: Particle Filters for Tracking Applications*. Boston, London: Artech House, 2004.

[10] D. Alspach and H. Sorenson, "Nonlinear Bayesian estimation using Gaussian sum approximation," *IEEE Trans. Aut. Contr.*, vol. 17, no. 4, pp. 439–448, 1972.

[11] E. W. Cheney, *Introduction to Approximation Theory*, 2nd ed. New York: Chelsea, 1982.

[12] W. Koch and M. Feldmann, "Cluster tracking under kinematical constraints using random matrices," *Robotics and Autonomous Systems*, vol. 57, no. 3, pp. 296 – 309, 2009.

[13] J. Koch, "Bayesian approach to extended object and cluster tracking using random matrices," *Aerospace and Electronic Systems, IEEE Transactions on*, vol. 44, no. 3, pp. 1042–1059, July 2008.

[14] M. Baum, M. Feldmann, D. Fränken, U. D. Hanebeck, and W. Koch, "Extended object and group tracking: A comparison of random matrices and random hypersurface models," in *LNCS*, 2010.

[15] D. Angelova and L. Mihaylova, "Extended object tracking using Monte Carlo methods," *IEEE Transactions on Signal Processing*, vol. 56, no. 2, pp. 825–832, 2008.

[16] M. Baum and U. D. Hanebeck, "Extended object tracking based on combined set-theoretic and stochastic fusion," in *Proc. of the International Conf. on Information Fusion*, 2009.

[17] M. Baum and U. Hanebeck, "Random hypersurface models for extended object tracking," in *Proc. of the IEEE International Symp. on Signal Processing and Information Technology (ISSPIT)*, 2009, pp. 178 –183.

[18] M. Baum, M. Feldmann, D. Fraenken, U. D. Hanebeck, and W. Koch, "Extended object and group tracking: A comparison of random matrices and random hypersurface models," in *GI Jahrestagung (2)*, 2010, pp. 904–906.

[19] J. Vermaak, N. Ikoma, and S. Godsill, "Sequential Monte Carlo framework for extended object tracking," *IEE Proc.-Radar, Sonar Navig.*, vol. 152, no. 5, pp. 353–363, 2005.

[20] F. L. Chernousko, *State Estimation for Dynamic Systems*. CRC Press, 1994.

[21] A. Kurzhanski and L. Vályi, "Ellipsoidal calculus for estimation and control," Birkh auser, Tech. Rep., 1997.

[22] S. Goldenstein, C. Vogler, and D. Metaxas, "Cue integration using affine arithmetic and gaussians," University of Pennsylvania, Tech. Rep., 2002.

[23] R. E. Moore, *Interval Analysis*. Englewood Cliffs, NJ: Prentice-Hall, 1966.

[24] L. Jaulin, M. Kieffer, O. Didrit, and E. Walter, *Applied Interval Analysis*. Springer-Verlag, 2001.

[25] L. Jaulin, "Nonlinear bounded-error state estimation of continuous-time systems," *Automatica*, vol. 38, no. 6, pp. 1079 – 1082, 2002. [Online]. Available: http://www.sciencedirect.com/science/article/B6V21-44SK0SM-1/2/07d95eca2656f1dafe65bc83def7894b

[26] A. Gning and P. Bonnifait, "Constraints propagation techniques on intervals for a guaranteed localization using redundant data," *Automatica*, vol. 42, no. 7, pp. 1167–1175, 2006.

[27] K. Gilholm and D. Salmond, "Spatial distribution model for tracking extended objects," *IEE Proc.-Radar, Sonar Navig.*, vol. 152, no. 5, pp. 364–371, 2005.

[28] O. C. Schrempf and U. D. Hanebeck, "A state estimator for nonlinear stochastic systems based on Dirac mixture approximations," in *ICINCO-SPSMC*, 2007, pp. 54–61.

[29] ——, "Recursive prediction of stochastic nonlinear systems based on Dirac mixture approximations," in *Proceedings of the American Control Conference*, 2007, pp. 1768–1774.

[30] F. Sawo, D. Brunn, and U. Hanebeck, "Parameterized joint densities with gaussian and gaussian mixture marginals," in *Proceedings of the 9th International Conf. on Information Fusion*, Florence, Italy, 2006.

[31] B. Noack, V. Klumpp, N. Petkov, and U. Hannebeck, "Bounding linearisation errors with sets of densities in approximate kalman filtering," in *Proc. of the 13th International Conf. on Information Fusion*. Edinburgh, UK: ISIF, 2010.

[32] Z. Khan, I. Gu, and A. Backhouse, "Robust visual object tracking using multi-mode anisotropic mean shift and particle filters," *Circuits and Systems for Video Technology, IEEE Transactions on*, vol. 21, no. 1, pp. 74 –87, jan. 2011.

[33] X. R. Li and V. Jilkov, "A survey of maneuveuvering target tracking. Part I: Dynamic models," *IEEE Trans. on Aerosp. and Electr. Systems*, vol. 39, no. 4, pp. 1333–1364, 2003.

[34] Y. Bar-Shalom and X. Li, *Estimation and Tracking: Principles, Techniques and Software*. Artech House, 1993.